Phase Behavior of Nylon 6/Trifluoroethanol/Carbon Dioxide Mixtures

S. J. Suresh, R. M. Enick, and E. J. Beckman*

Department of Chemical and Petroleum Engineering, University of Pittsburgh, Pittsburgh, Pennsylvania 15260

*Received June 10, 1993; Revised Manuscript Received October 28, 1993**

ABSTRACT: The phase behavior of the ternary system Nylon 6/2,2,2-trifluoroethanol/CO_2 has been examined at 298.15, 318.15, and 373.15 K and pressures up to 40 MPa. The ternary system exhibits solid-liquid-vapor equilibrium at 298.15 and 318.15 K and liquid-liquid-fluid equilibrium at 373.15 K. At 298.15 and 318.15 K and 10.34 MPa, a metastable equilibrium exists and the time for phase separation depends on the Nylon 6 composition and temperature. CO_2 behaves as a useful diluent for the Nylon 6/TFEtOH mixture at Nylon 6 concentrations below 4 wt %, as large amounts of CO_2 can be added while maintaining a reasonable Nylon 6 solubility. At 373.15 K, the ternary system exhibits liquid-liquid instability and CO_2 behaves as an excellent diluent in two regions: (1) region with a high Nylon 6 concentration, where a small amount of CO_2 can enhance the Nylon 6 solubility in TFEtOH; (2) region with a low Nylon 6 concentration, similar to the results obtained at 298.15 and 318.15 K. The acquired experimental data are correlated using two state-of-the-art theoretical models: (1) SAFT and (2) Sanchez-Lacombe-Perram equation of state.

Introduction

Polyamides exhibit strong intermolecular and intramolecular hydrogen-bonded networks,[25] and thus disruption of these hydrogen bonds is necessary to dissolve these materials. Solvents most likely to swell or dissolve polyamides are, consequently, compounds that exhibit a strong tendency to hydrogen bond with the amide hydrogen and the carbonyl oxygen atoms. Unfortunately, such solvents often either have high boiling temperatures,[41] such as *m*-cresol, or are highly reactive,[4] such as sulfuric acid, and thus tend to degrade the polymer. An alternative to these solvents is 2,2,2-trifluoroethanol (TFEtOH), which is known to dissolve Nylon 6.[23] Recently, Aharoni et al.[1] showed that TFEtOH/chloroform mixtures are excellent mixed solvents for Nylon 6, with chloroform exhibiting a cosolvent behavior. Unfortunately, TFEtOH is expensive, is relatively toxic, and forms highly viscous solutions with Nylon 6, while chloroform poses environmental hazards owing to its chlorine content.

Given this background, we are exploring the effects upon polyamide solubility of adding a low-boiling, nontoxic, and inexpensive diluent, CO_2 in this case, to TFEtOH. We anticipate that the addition of CO_2 will lower the viscosity, solvent critical temperature, and cost, while maintaining a relatively high solubility of Nylon 6 in the resulting mixed solvent. CO_2 in its supercritical state exhibits a viscosity from 0.01 to 0.1 cP, and, because the increase in the viscosity of a liquid due to the addition of polymer is relative to the pure fluid, use of CO_2 as a solvent generally results in lower solution viscosities than analogous liquid solutions. Further, use of a solvent above its liquid-vapor critical temperature (T_c) also includes certain advantages. For example, removal of a supercritical solvent can be achieved through pressure reduction, avoiding the liquid-vapor phase boundary and thus minimizing condensation/residual solvent in the precipitated polymer. In this study, we have measured the phase boundaries for the Nylon 6/TFEtOH/CO_2 system at temperatures from 298 to 373 K and pressures to 40 MPa.

In addition to experimental studies, theoretical analysis of the phase behavior of complex systems is also useful for obtaining fundamental insights at the molecular level. The significant features of the Nylon 6/TFEtOH/CO_2 system that need to be reproduced by a theoretical model are the presence of (a) molecules with large size differences, (b) different types of molecular association, such as those present in the self-association of TFEtOH, self-association of Nylon 6, and cross-association between TFEtOH and Nylon 6, (c) solutions under high pressures involving compressible fluids, and (d) multiphase equilibria, for example, solid-liquid-liquid-fluid equilibrium.

Many methods have been proposed to correlate the phase behavior of polymer solutions. Notable among recent models is the Sanchez-Lacombe equation of state,[38,39] developed for mixed molecular fluids of arbitrary geometries and sizes, but which do not contain any molecular association. Since then, several attempts have been made to modify the Sanchez-Lacombe equation to incorporate association effects (for example, see refs 32-34). Recently, a significant step in this direction was made by Panayiotou and Sanchez,[35] who incorporated the Perram-Veytsman theory[44] of hydrogen bonding into the original Sanchez-Lacombe equation of state. Veytsman,[44] invoking arguments originally proposed by Levine and Perram,[27] theorized that the properties of a hydrogen-bonded fluid depended on the number of arrangements of hydrogen bonds in the system but not on the distribution of the associates. By incorporating the Perram-Veytsman theory in the context of the Sanchez-Lacombe equation of state, Panayiotou and Sanchez[35] showed that such an argument yields considerable accuracy in the representation of phase equilibria in hydrogen-bonded fluids. This modified version of the Sanchez-Lacombe equation of state will be referred to as the Sanchez-Lacombe-Perram (SLP) equation in this paper.

We have also evaluated another recent equation of state for polyatomic molecules, SAFT,[21,22] which incorporates three types of interactions among molecular segments: (1) hard-sphere and attractive dispersion interactions, developed by Carnahan and Starling[5] and Alder et al.,[2] respectively; (2) covalent bonding in chain molecules;[6] (3) specific interactions based on the theory developed by

* Abstract published in *Advance ACS Abstracts*, December 15, 1993.

0024-9297/94/2227-0348$04.50/0

Wertheim,[46-49] who analyzed the grand canonical partition function in terms of cluster diagrams and deduced simple, closed-form expressions for the free energy of association. Wertheim's theory has been shown to provide accurate phase equilibrium correlations for a variety of associating molecules, including alcohols, water, ketones, hydrocarbons, and H_2S.[7,21,22,42] Wertheim's theory neglects the formation of ring structures, yet in molecules such as water and polyatomic fluids with multiple association sites, rings can form easily. However, simulation studies for water[14,24,30] and methanol[24,30] indicate that Wertheim's theory accurately calculates several thermodynamic properties, such as internal energy, pressure, and distribution of H-bonded clusters, despite the lack of incorporation of ring structures in the model. Wertheim's theory is very similar to the Perram–Veytsman theory[10] with one key difference: the dependence of the association strength on temperature and density differs for the two theories.

Theory

The SAFT and SLP models possess three important types of molecular interactions: (1) repulsive, (2) dispersion, and (3) association effects. Due to the significance of H bonding in the Nylon 6/TFEtOH/CO_2 system, this section primarily focuses on the association theories that have been adopted by the SAFT and SLP models, i.e., Wertheim's theory and the Perram–Veytsman theory. A detailed explanation of the repulsive and the dispersion contributions of chain molecules to equations of state can be obtained elsewhere.[21,22,35,38,39]

Wertheim's theory and the Perram–Veytsman theory are in many ways similar to each other,[10] although they have been derived differently. While Wertheim used cluster diagrams to solve for the grand canonical partition function of associating systems, Perram–Veytsman theory focuses on determining the number of hydrogen bonds, by minimizing the free energy of the system. Differences and similarities between the two theories are explained below in detail.

We consider a simple system: pure Nylon 6 with n proton donor and n proton acceptor sites. Let us also assume that the CO–H and NH–O hydrogen-bond energies are equal to each other and can be represented by an average energy. Both Wertheim's theory and Perram–Veytsman theory (the latter as implemented by Panayiotou and Sanchez[35]) give the same expression for the mole fraction of molecules *not bonded* at the bonding site A.

$$X_A = \frac{2}{1 + (1 + 4nN_{Av}\rho\Delta)^{1/2}} \tag{1}$$

where Δ is the association strength and is given in Wertheim's theory[21]

$$\Delta = K\sigma^3 g^{(\sigma)}[\exp(-H^\circ/RT) - 1] \tag{2}$$

where $g^{(\sigma)} \equiv$ pair correlation function at contact $= (1 - \eta/2)/(1 - \eta)^3$, $\eta \equiv$ reduced density $= \rho m\pi d^3 N_{Av}/6$, $m \equiv$ number of segments, $\sigma \equiv$ temperature-independent segment diameter, $d \equiv$ effective temperature-dependent segment diameter, $\rho \equiv$ bulk fluid density, $K \equiv$ dimensionless bonding volume, $H^\circ \equiv$ enthalpy of hydrogen-bond formation, $R \equiv$ gas constant, $T \equiv$ temperature, and $N_{Av} \equiv$ Avogadro's number.

Since the segment volume, $v^{\circ\circ}$, is defined as follows:

$$v^{\circ\circ} = \Pi N_{Av}\sigma^3/6\tau \tag{3}$$

where $\tau = 0.740\,48$, eq 2 becomes

$$\Delta = Kv^{\circ\circ}(6\tau)/(\Pi N_{Av}) g^{(\sigma)}[\exp(-H^\circ/RT) - 1] \tag{4}$$

or

$$\Delta = K^1 v^{\circ\circ}[\exp(-H^\circ/RT) - 1] \tag{5}$$

where

$$K^1 = 6K\tau g^{(\sigma)}/\Pi N_{Av} \tag{6}$$

It should be noted that $g^{(\sigma)}$ and K^1 are functions of the fluid density.

For the Perram–Veytsman theory,[35] the association strength is given as follows:

$$\Delta = Kv^*[\exp(-(H^\circ + PV^\circ)/RT)] \tag{7}$$

where $K = \exp[S^\circ/R]$, $v^* \equiv$ segment volume, $V^\circ \equiv$ volume change on hydrogen-bond formation, $S^\circ \equiv$ entropy change on hydrogen-bond formation, and $P \equiv$ pressure in the system.

The Helmholtz free energy of association (for both theories) is given by:

$$A_{bond} = 2n \ln(x_A) + n(1 - X_A) \tag{8}$$

There are several points worth noting based on the above observations:

(1) It is striking to note the similarities between the two theories although Wertheim's theory excludes the formation of rings, while no such limiation seems "apparent" in the Perram–Veytsman theory, since the latter focuses on the bond-counting approach and hence does not distinguish between linear, tree, and ring structures.

(2) It is clear from the above expressions that although the dependence of the free energy of association, A_{bond}, on the association strength, Δ, is identical for both theories (eq 8), the dependence of the association strength on temperature and density differs (eqs 5 and 7). In particular, derivation of eq 7 requires the evaluation of the probability of bond formation (P_{ij}) between a specific proton donor and a specific proton acceptor group. This probability was calculated by accounting for two factors: (1) spatial proximity of the H-bond sites, which was assumed to be proportional to the volume of the acceptor group divided by the total system volume, rather than rigorously calculating the bonding volume, and (2) spatial orientation, steric considerations, and loss of rotational degrees of freedom, which was assumed to be proportional to $\exp[S^\circ/R]$ and, debatably, independent of the fluid density. Wertheim's derivation, on the other hand, does not include such assumptions.

Thus, certain assumptions invoked in the association contribution of SLP are debatable. Similar arguments apply for mixtures that include multiple associating species. For example, Gupta et al.[15] showed that more complex expressions are needed for P_{ij} and the density dependence of eq 7 to mimic FTIR results for associating solvent–supercritical fluid systems. Despite the limitations in the theories, *both models* have been shown to be quite successful in representing the phase behavior of a number of associating systems.[22,35] However, the representation of *multiphase* equilibria of associating polymer solutions at high pressures, such as the Nylon-6/TFEtOH/CO_2 system, still remains a challenge for both models. In this study, we will evaluate the performance of both SLP and SAFT in the description of multiphase equilibria, while attempting to generate the model parameters from independent soures, to minimize the amount of data-fitting required.

For the evaluation of phase equilibrium properties using equations of state at pressure P, the following equations have been used.

Liquid–liquid equilibrium:

$$f_i^{L1} = f_i^{L2} \tag{9}$$

Solid–liquid equilibrium:

$$\ln \frac{f_i^L}{f_i^{Lo}} = -\frac{\Delta H_f}{RT}\left[1 - \frac{T}{T_m}\right] + \frac{\Delta C_{pf}}{R}\left[\frac{T_m - T}{T} + \ln \frac{T}{T_m}\right] - \frac{(V_i^L - V_i^S)(P - P_i^{sat})}{RT} \tag{10}$$

where f_i^L and f_i^{Lo} are the fugacity of component i in a mixture and pure state, respectively, ΔH_f and ΔC_{pf} are the changes in enthalpy and specific heat of component i due to fusion at its normal melting point temperature T_m, V_i^L and V_i^S are the specific volumes of liquid and solids, and P_i^{sat} is the saturated vapor pressure of component i at temperature T.

Procedure To Obtain Model Parameters

Each molecule of TFEtOH and each repeat unit of Nylon 6 were assigned one proton donor and one proton acceptor group. The pure-component parameters for TFEtOH for both models were determined by fitting the model equations of state to vapor pressure data (obtained in this study) at temperatures from $T_r = 0.5$ to 0.9 ($T_r = T/T_c$), plus knowledge of the liquid density at 298.15 K and 0.1 MPa. The pure-component parameters of Nylon 6 were obtained by fitting the liquid density data[4,28] at pressures from 0.1 to 200 MPa and temperatures from 493 to 593 K. The number-average molecular weight was taken to be 6000.0, as indicated by the supplier. Effects of polydispersity on the phase equilibrium properties were neglected in this study. In addition to PVT data, the fusion properties of Nylon 6 are essential for evaluating the SLE of the Nylon 6/TFEtOH/CO_2 system. The heat of fusion (21.47 kJ/mol) was obtained from Brandrup and Immergut,[4] the melting point temperature (501.65 K) from the supplier, and the specific heat of fusion (60.0 J/mol K) from Gaur et al.[13] and Xenopoulos and Wunderlich.[50] The pure-component parameters of CO_2 were obtained by fitting appropriate model equations of state to the saturated liquid density and the vapor pressure data[9] at temperatures from $T_r = 0.5$ to 0.9.

The association parameters of the hydrogen bonds formed between TFEtOH and Nylon 6 are essential to both models for the evaluation of phase equilibrium properties of Nylon 6/TFEtOH mixtures. Unfortunately, the NH–O and CO–H hydrogen-bond parameters between Nylon 6 and TFEtOH and not known unambiguously[12] and hence have to be treated as adjustable parameters. However, to minimize the number of adjustable parameters in this study, the properties of the NH–O and CO–H hydrogen bonds are assumed to be equal to each other, and these parameters have been approximated from the pure-component properties of Nylon 6 and TFEtOH, as follows:

$$H^\circ_{ij} = (H^\circ_{ii} + H^\circ_{jj})/2 \tag{11}$$

$$K_{ij} = (K_{ii} + K_{jj})(1 - a_{ij})/2 \tag{12}$$

$$V^\circ_{ij} = (V^\circ_{ii} + V^\circ_{jj})/2 \tag{13}$$

where H° is the enthalpy of the H bond, K is the dimensionless bonding volume (Wertheim's theory) or exp[S°/R] (Perram–Veytsman theory), V° is the change in volume due to H-bond formation, j is a site in molecule 2 cross-associating with site i in molecule 1, and a_{ij} is a parameter that adjusts the degree of cross-association between Nylon 6 and TFEtOH. As examples, if the value of a_{ij} is unity, the bonding volume of a cross-associated hydrogen bond is zero and, hence, there is no cross association between the two molecules; if a_{ij} is zero, the bonding volume of the cross-associated hydrogen bond is simply the arithmetic mean of the bonding volumes of the self-associated hydrogen bonds of the two molecules. It should be noted that for cross-associated networks, accurate combining rules for the hydrogen-bond properties have not yet been developed[45] and, hence, eqs 11–13 are empirical and may not be valid in general.

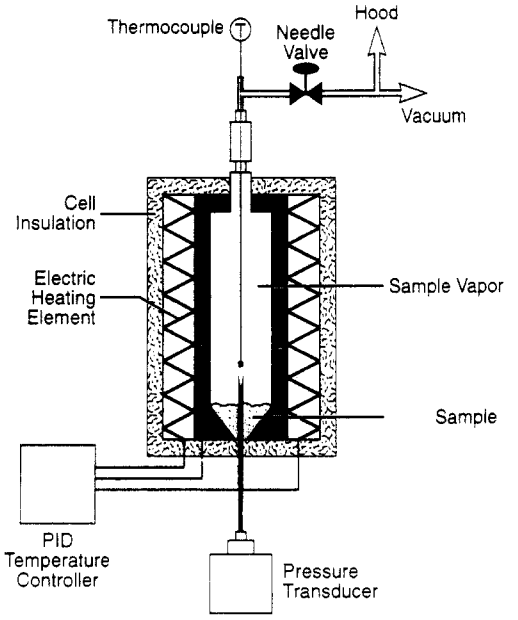

Figure 1. Vapor pressure apparatus.

Experimental Section

Materials. Nylon 6[1] and NMR-grade TFEtOH (99.5%) were purchased from Aldrich. CO_2 (bone-dry) was received from Linde division of Union Carbide Corp. and used without further purification.

To study the effect of adding CO_2 on the phase equilibrium properties of the Nylon 6/TFEtOH system, we performed phase equilibrium experiments on the following mixtures: (a) TFEtOH, vapor pressure (vapor–liquid); (b) Nylon-6/TFEtOH, solid–liquid equilibrium (SLE); (c) TFEtOH/CO_2, liquid densities; (d) Nylon 6/CO_2, solid–fluid equilibrium (SFE); (e) Nylon 6/TFEtOH/CO_2, solid–liquid–liquid–fluid equilibrium (SLLFE).

This section explains the experimental apparatus and the methods followed in performing the various types of phase equilibrium analyses involved in the above systems.

Since the vapor pressure and the critical point data for TFEtOH were not available in the literature, we measured these quantities in our laboratory. The vapor pressure experiments were conducted in a 50-cm^3 apparatus (Figure 1), constructed from A286 superalloy (Fluitron Inc.). A thermocouple, calibrated with an NBS thermometer, is placed directly in the sample volume. The apparatus is heated by a heating element, the temperature of which is maintained to within 1 K by a PID controller. The pressure transducer is calibrated against a Heise gauge with a resolution of 0.1 psia and an accuracy of ±1.0 psia. In a typical experiment, a known mass of TFEtOH was placed in the sample space, vacuum was applied to remove traces of air, and the apparatus was sealed. The sample was then heated to the required temperature, and after allowing a sufficient period of time for the pressure in the apparatus to stabilize, the vapor pressure was

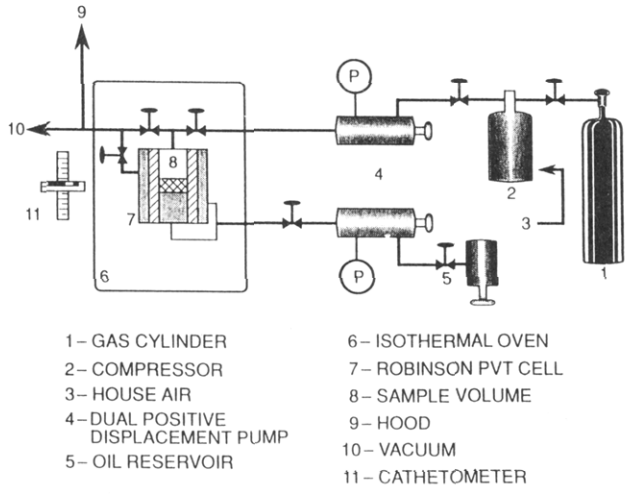

Figure 2. High-pressure phase equilibrium apparatus.

noted. The temperature above which the pressure started deviating from the vapor pressure curve provided the critical point data.

The high-pressure solid–liquid equilibrium (SLE) data of the Nylon 6/TFEtOH system was obtained by melting point depression analysis, performed in a differential scanning calorimeter (DSC; TA Instruments, 10°/min scan rate). In a typical experiment, a known amount of Nylon 6 was added to the DSC pan and then sealed in a vial above liquid TFEtOH. After varying lengths of time, the sample was removed from the saturated TFEtOH atmosphere, weighed, sealed, and then inserted into the high-pressure chamber of DSC. The melting temperature of the swollen polymer was subsequently obtained from the DSC scan, under a nitrogen pressure of 6.55 MPa to inhibit the evaporation of TFEtOH at high temperatures (the sample was weighed after each run to ensure that no TFEtOH had been lost).

For obtaining low-pressure solubility data of Nylon 6 in TFEtOH at temperatures below the boiling point of TFEtOH, several mixtures with varying, but closely spaced, Nylon 6 compositions were prepared in separate bottles. These bottles were immersed in a constant-temperature oil bath. The contents in each bottle were mixed using magnetic stirrers and the transparencies of the samples were observed after a sufficient period of time. The onset of a cloudy appearance in a particular sample provided the solubility data.

The high-pressure phase equilibrium experiments (SLE, SFE, and SLLFE) on Nylon 6/TFEtOH/CO_2 systems were performed in a visual, variable-volume cell (D. B. Robinson and associates), as shown in Figure 2. The details of this apparatus are given by Hoefling et al.[20] In brief, the cell contains a quartz tube, in which resides a floating piston that separates the fluid of interest and an overburdened fluid, in this case silicone oil. The pressure on the sample can be varied by withdrawing/pumping the overburdened fluid to adjust the position of the piston. The cell is itself encased in an oven for attaining specified temperatures. Mixing of the cell components is performed via the addition of steel spheres and the subsequent rocking of the cell. Liquid–liquid equilibrium (LLE) cloud-point pressures are visually observed by compressing/expanding the fluid of interest and observing the transparency of the mixture. The solid–liquid equilibrium (SLE) cloud points are determined by visually observing the onset of solid particle formation. Sampling of the various phases cannot currently be performed using this apparatus. In a typical high-pressure experiment, a known mixture of Nylon-6/TFEtOH was loaded into the cell. The mixture was compressed by injecting the over burdened fluid using a Ruska reciprocating pump. The oven was stabilized at the temperature of interest, and the cell was rocked to dissolve the Nylon 6. Known amounts of compressed CO_2 were subsequently added to the cell using another Ruska reciprocating pump, which is calibrated to read displaced volumes (the liquid density data were obtained from ref 43). The compositions of the various species were calculated from the known injected weight of CO_2 and the initial

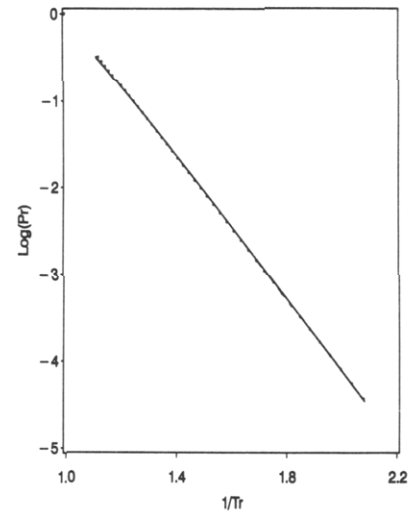

Figure 3. Reduced vapor pressure (P_r) curve at different reduced temperatures (T_r) for TFEtOH: (○) eq 14; (—) SAFT correlations; (– –) SLP correlations.

Table 1. Pure-Component Molecular Parameters for SAFT[a]

	v^{oo} (cm^3)	U_0/k (K)	m	K	H^o (kJ/mol)	e/k
CO_2	13.578	216.08	1.417	0.000	0.0	40.0
TFEtOH	25.201	215.01	1.513	0.025	−24.942	10.0
Nylon 6	25.684	225.00	110.475	0.001	−35.750	10.0

[a] v^{oo} ≡ temperature-independent segment volume, U_0 ≡ square well-potential energy well-depth, m ≡ number of segments, K ≡ dimensionless bonding volume, H^o ≡ enthalpy of the hydrogen bond, e/k ■ constant related to Pitzer's acentric factor and critical temperature, and k ≡ Boltzmann's factor.

weights of Nylon 6 and TFEtOH placed in the cell. The cell was then rocked for a few minutes and subsequently checked for phase separation.

Liquid densities of the TFEtOH/CO_2 binary system were obtained by inserting glass beads with known densities, calibrated to within an error of 0.0001 g/cm^3 (Techne Inc.), into the cell. Initially, TFEtOH was loaded into the cell. Subsequently, CO_2 was slowly added, and the positions of the beads were noted. The density of the bead that was located in the center of the cell provided the liquid density for the mixture, whose composition was calculated from the initial amount of TFEtOH and the amount of CO_2 added.

Results and Discussion

The experimental vapor pressure curve of TFEtOH is shown in Figure 3. A plot of $\log(P_r^{sat})$ vs $1/T_r$ is a straight line with the equation

$$\log(P_r^{sat}) = 4.1262 - 4.1126/T_r \qquad (14)$$

Equation 14 fits the vapor pressure curve to an accuracy of 0.7% absolute deviation. The critical constants of TFEtOH have been measured to be:

$$P_c = 4.27 \text{ MPa}$$

$$T_c = 490.2 \text{ K}$$

The critical temperature obtained from our experiment agreed well with the group contribution prediction of Eduljee,[36] which provided a value of 492.42 K for T_c.

The pure-component parameters for Nylon 6, TFEtOH, and CO_2 for SAFT and SLP are given in Tables 1 and 2, respectively. Our value of the hydrogen-bond enthalpy (−24.94 kJ/mol) for TFEtOH falls within the range of −12.0 to −33.0 kJ/mol reported in the literature.[23] One must note that, although numerous data on the thermodynamic

Table 2. Pure-Component Molecular Parameters for SLP[a]

	T^* (K)	P^* (MPa)	ρ^* (mol/cm^3)	S° (J/(K·mol))	H° (kJ/mol)	V° (cm^3/mol)
CO_2	290.7	675.03	0.036 200	0.00	0.00	0.00
TFEtOH	489.7	218.56	0.015 530	-26.50	-24.942	-5.60
Nylon 6	550.0	160.00	0.000 224	-52.05	-37.750	-3.74

[a] T^*, P^*, and ρ^* are the molecular parameters of the physical contributions (repulsive and dispersion effects) to the free energy. H°, S°, V° ≡ enthalpy, entropy, and volume changes on hydrogen-bond formation.

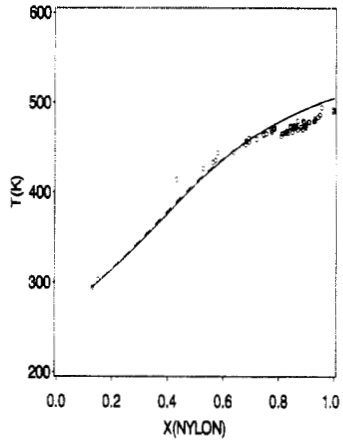

Figure 4. Solid–liquid equilibrium curve (weight fraction Nylon 6 vs temperature) for the Nylon 6/TFEtOH mixture at 6.55 MPa: (O) experimental data; (—) SAFT correlations; (- -) SLP correlations.

functions of the OH–O hydrogen bond exist in the literature,[37] they often disagree with each other and cannot be unambiguously used. The hydrogen-bond enthalpy for Nylon 6 in our study has been determined to be -35.75 kJ/mol. The hydrogen-bond enthalpies of a number of polyamides have been previously reported[12,29,40] to be in the range from -29.0 to -50.0 kJ/mol; thus our value is quite reasonable.

Table 3 shows that SAFT and SLP provide an accurate representation of the pure-component properties of Nylon 6, TFEtOH, and CO_2. Figure 3 shows a comparison of the experimental vapor pressure correlation (eq 14) with the model correlations for TFEtOH.

The solubility of Nylon 6 in CO_2 was found to be negligible (unmeasurable using our equipment) at temperatures from 298.15 to 373.15 K and pressures ranging from 0.1 to 40 MPa, a result which can be attributed to the absence of strong association sites in CO_2 that can rupture the interchain hydrogen bonds present in Nylon 6. The solubility and melting point depression curves for the Nylon-6/TFEtOH mixture (Figure 4) suggest that TFEtOH is an excellent solvent for Nylon 6 at temperatures above 298.15 K. The formation of highly viscous solutions caused the following problems:

(1) The solubility data for temperatures above 313 K could not be measured.

(2) The potential presence of a liquid–liquid phase separation envelope could not be experimentally investigated.

It should be noted that the solution viscosity depends on two major factors: (1) temperature, (2) composition. Hence, although the viscosity of a solution at a given composition is expected to decrease with increasing temperature, the increased Nylon 6 solubility at higher temperatures causes an increase in the viscosity. The solid–liquid equilibrium analysis for SAFT and SLP provided a good correlation with the experimental data (Figure 4). A single parameter, a_{ij} (Table 4), which controls the extent of cross-association between Nylon 6 and TFEtOH, was adjusted to fit the SLE data. Note that the Nylon 6/TFEtOH binary parameter (k_{ij}) was set to zero and hence was not adjusted. Neither model indicated liquid–liquid phase separation for the Nylon 6/TFEtOH binary over the temperature range of 298–493 K.

Before proceeding to the ternary Nylon-6/TFEtOH/CO_2 system, we analyzed the TFEtOH/CO_2 system. At low pressures, vapor and liquid phases coexist, and at pressures above the bubble point pressure, the vapor phase vanishes. We checked for phase separation/instability in the liquid phase. We found that CO_2 was completely miscible in TFEtOH at temperatures between 298 and 373 K and pressures ranging from 0.1 to 40 MPa, despite the fact that the fluorine atoms in TFEtOH increase its tendency to self-associate as compared to ethanol, which is completely miscible in CO_2.[11] This result can probably be based on recent observations that fluorinated functional groups ($-CF_2$) interact more favorably with CO_2 than the corresponding alkyl groups ($-CH_2$).[20] Both models, SLP and SAFT, do not indicate a liquid–liquid phase separation for this system.

The experimental data and model predictions of the liquid densities for this system at 295.15 K and 6.98 MPa are shown in Figure 5. It is clear that both models are equally accurate. The binary interaction parameter (k_{ij}) for the TFEtOH/CO_2 system for each model is shown in Table 4. It should be noted that while the k_{ij} parameter is substantially negative for SLP, its value for SAFT is positive but close to zero. This trend was observed for mixtures containing CO_2 and other alcohols as well. For example, Figure 6 shows a plot for the CO_2/methanol system at 298.15 K with a k_{ij} value of -0.23 for the SLP model and 0.01 for SAFT. However, our analysis for other associating mixtures involving water, ketones, alcohols, haloforms, hydrocarbons, etc., but not including CO_2, shows that the k_{ij} parameter for the SLP model is close to zero. Hence, it is possible that the SLP model is indicating some cross-association between CO_2 (a weak Lewis acid) and alcohols, thus yielding a negative interaction parameter as a result of an artificial enhancement in the attractive dispersion energy, due to the lack of incorporation of any cross-association effects with CO_2 in the model. Such cross-association effects have been investigated over the years, producing evidence that CO_2 forms weak complexes with alcohols, and oxygen-containing compounds in general, in condensed mixtures of these substances[3,18,19] and, more recently, in the gas phase as well.[8,16,17]

The Nylon 6/TFEtOH/CO_2 system was analyzed at 298.15, 318.15, and 373.15 K. At 298.15, and 318.15 K, the ternary mixtures exhibited SLE at pressures above the bubble point pressure (i.e., the transition from solid–liquid–vapor to solid–liquid equilibria) of the mixture. The effect of pressure on solid–liquid equilibrium was found to be insignificant and hence could not be accurately determined. For example, the solubility of Nylon 6 in a 2:1 (weight ratio) TFEtOH/CO_2 mixture at 318.15 K was found to increase from 8.48% to 8.89% upon increasing the pressure from 10 to 35 MPa. This feature is probably due to the fact that liquids show small increases in density with pressure. However, an interesting feature of this system is that the apparent SLE boundary of the ternary mixture was found to shift if sufficient time was provided between CO_2 injections, as seen in Figure 7. The metastable condition existed for periods as long as 10 h bfore the onset of gelation/phase separation. The time for

Table 3. Percent Average Absolute Deviation in Pure-Component Properties

	density			vapor pressure		
	range	SAFT	SLP	range	SAFT	SLP
Nylon 6	T = 493 – 593 K, P = 0–200 MPa	3.9%	3.3%			
TFEtOH	T = 298 K, P = 0.1 MPa	0.0%	0.0%	T = 245–441 K	2.8%	2.2%
CO_2	T = 153–275 K, $P = P^{sat}$	1.7%	1.6%	T = 153–275 K	1.2%	1.3%

Table 4. Values of Adjustable Parameters for SAFT and SLP

	k_{ij}		a_{ij}	
	SAFT	SLP	SAFT	SLP
Nylon 6/TFEtOH	0.00	0.00	0.18	0.115
Nylon 6/CO_2	0.15	–0.38	1.00	1.000
TFEtOH/CO_2	0.07	–0.28	1.00	1.000

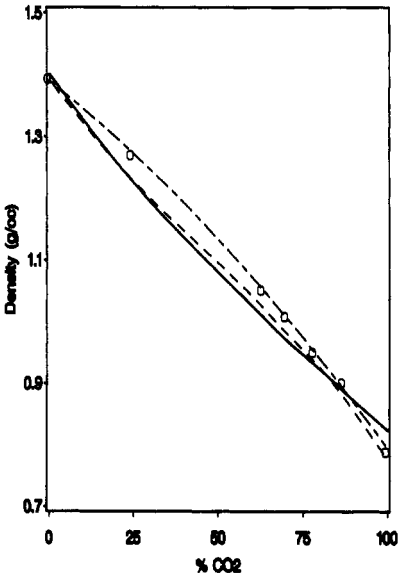

Figure 5. Liquid density of TFEtOH/CO_2 mixtures (weight basis) at 298.15 K and 6.98 MPa: (O, - · -) experimental data; (—) SAFT correlations; (– –) SLP correlations.

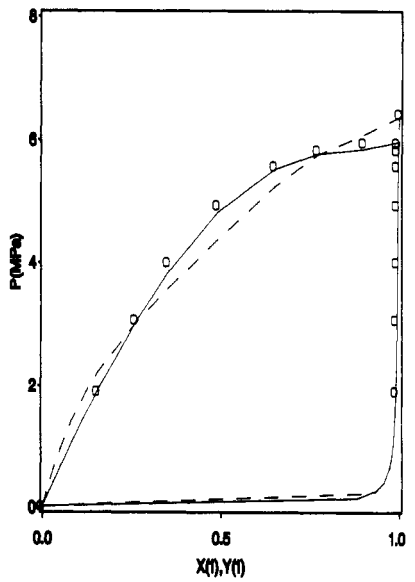

Figure 6. Vapor–liquid equilibrium curve for the CO_2 (1)/methanol (2) system (mole fraction CO_2 vs pressure) at 298.15 K: (O, - · -) experimental data;[31] (—) SAFT correlations; (– –) SLP correlations.

gelation/separation depended on both the polyamide composition and temperature. Although mixed solvents have been known to form more gel-resistant solutions than single solvents,[25] the TFEtOH/CO_2 solvent mixture tended to form "gels" more readily than TFEtOH in the presence

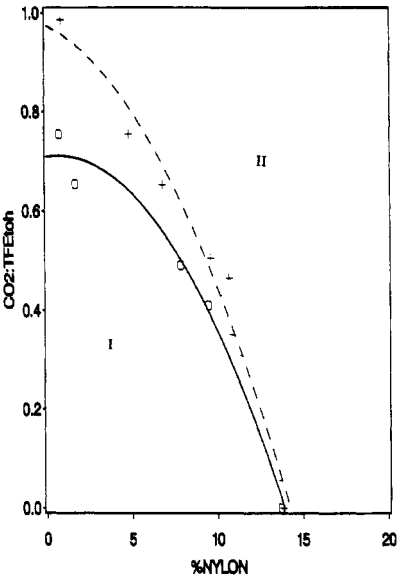

Figure 7. Solid–liquid equilibrium curve (weight basis) for the Nylon 6/TFEtOH/CO_2 system at 10.34 MPa and 298.15 K: (+, – –) curve observed when time between CO_2 injections is 15 min; (O, —) curve observed when time between CO_2 injections is 600 min. Region I consists of a single liquid phase. Region II consists of two phases (solid–liquid).

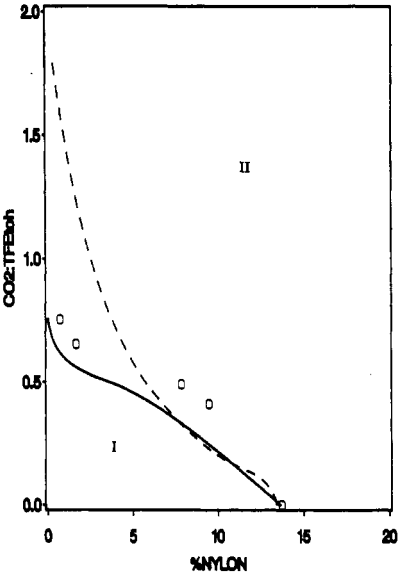

Figure 8. Solid–liquid equilibrium curve (weight basis) for the Nylon 6/TFEtOH/CO_2 system at 10.34 MPa and 298.15 K: (O) experimental data; (—) SAFT correlations; (– –) SLP correlations. Region I consists of a single liquid phase. Region II consists of two phases (solid–liquid).

of Nylon 6. One possible explanation of this phenomenon can be based on the slow nucleation and growth of the crystals, which in turn might be attributed to the high strength of H bonds formed between Nylon 6 and TFEtOH. Figures 8 and 9 show SLE plots for the Nylon 6/TFEtOH/CO_2 solutions at 298.15 and 318.15 K and 10.34 MPa. We believe that these plots represents the "true" phase boundaries (time between CO_2 injections was set at 10 h) and not the metastable conditions. An interesting feature of the plots is the steep increase in the CO_2:

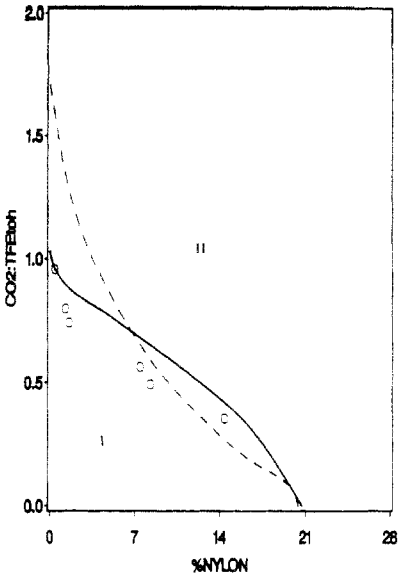

Figure 9. Solid–liquid equilibrium curve (weight basis) for the Nylon 6/TFEtOH/CO_2 system at 10.34 MPa and 318.15 K: (○) experimental data; (—) SAFT correlations; (– –) SLP correlations. Region I consists of a single liquid phase. Region II consists of two phases (solid–liquid).

TFEtOH weight ratio with decreasing Nylon 6 composition, especially in the region below 4 wt % Nylon 6. The result implies that adding a small amount of TFEtOH to pure CO_2 improves the solubility of Nylon 6 by orders of magnitude in this region.

The model correlations for the Nylon 6/TFEtOH/CO_2 mixtures at 298.15 and 318 K are shown in Figures 8 and 9. Although the ternary system requires three adjustable parameters, the TFEtOH/CO_2 and Nylon 6/TFEtOH binary parameters were obtained from binary analysis (Table 4). Since the solubility of Nylon 6 in CO_2 was found to be negligible, we could not obtain the interaction parameter for this pair from binary analysis. Hence, only the Nylon 6/CO_2 interaction parameter (k_{ij}) was adjusted for both models to provide a good fit of the ternary solid–liquid equilibrium data. The important features of the models are as follows:

(a) While SAFT performs satisfactorily at both temperatures over the whole range of compositions, SLP overestimates the solubility of Nylon 6 in TFEtOH/CO_2 mixtures at low Nylon 6 concentrations.

(b) The SLP model suggests an increase in the solubility of Nylon 6 in TFEtOH upon the addition of small quantities of CO_2 at 298.15 and 318.15 K, i.e., a *cosolvent effect* by CO_2, as indicated by a change in curvature at high Nylon 6 concentrations. Such cosolvent effects have been experimentally observed with other diluents, such as chloroalkanes.[1] Unfortunately, the cosolvent effect in our study could not be experimentally verified due to high solution viscosity at high Nylon 6 concentrations. A possible explanation for the cosolvent phenomena exhibited by SLP is that solvent–polymer interactions are preferred to solvent–solvent interactions at low concentration of one of the solvents.[26] In other words, the contact between molecules of two solvents is discouraged, hence encouraging the preferential solvation of Nylon 6 by the two solvents. To confirm this phenomenon for SLP, we performed a sensitivity study on the TFEtOH/CO_2 binary interaction parameter (k_{ij}). A decrease in the k_{ij} parameter for the TFEtOH/CO_2 pair below its value obtained from the binary analysis (Table 4) caused a reduction in the cosolvent effect. In other words, increasing the attractive dispersion energy for the TFEtOH/CO_2 pair caused an increase in the solvent–solvent interactions, thereby deteriorating the cosolvent effect.

(c) SAFT predicts that CO_2 is a good diluent, but not a cosolvent, for the Nylon 6/TFEtOH system.

In summary, the SLP model is inaccurate at low Nylon 6 concentrations and predicts CO_2 to be a cosolvent at high Nylon 6 concentrations. On the other hand, SAFT is accurate over the whole range of experimentally studied Nylon 6 concentrations and predicts that CO_2 is a good diluent, but not a cosolvent. Unfortunately, at high Nylon 6 concentrations, due to viscosity problems, experimental data could not be obtained to verify the predictions of the two models.

At 373.15 K, the Nylon 6/TFEtOH/CO_2 mixtures did not exhibit SLE at any of our experimental conditions. Instead, liquid–liquid phase separation was observed. At low CO_2 content and pressures below the bubble point pressure, two phases were observed: a TFEtOH-rich liquid phase in equilibrium with a CO_2-rich fluid phase. As the CO_2 content in the system increased, three phases were observed: two liquid phases and a fluid phase. Above the bubble point pressure, liquid–liquid equilibrium was observed. As the pressure was further increased, the liquid–liquid cloud point appeared (Table 5).

Figure 10 shows a plot of the experimental liquid–liquid equilibrium (LLE) phase surface for the ternary system at 373.15 K. As expected, the liquid–liquid cloud-point pressure increases with increasing CO_2 concentration at constant Nylon 6 concentration. One might also expect that the allowable amount of CO_2 in the single-phase region would decrease with increasing Nylon 6 concentration at constant pressure, given that CO_2 is a poor solvent for

Table 5. Liquid–Liquid Cloud-Point Pressure for Nylon 6/TFEtOH/CO_2 Mixtures at 373.15 K

Nylon 6 wt %	TFEtOH/CO_2 wt ratio	pressure (MPa)	Nylon 6 wt %	TFEtOH/CO_2 wt ratio	pressure (MPa)
3.67	1.652	14.48	10.45	1.966	17.59
3.49	1.443	19.31	10.03	1.729	22.41
3.34	1.304	23.45	9.64	1.538	26.55
3.20	1.173	29.65	9.28	1.389	32.07
3.09	1.091	33.10	11.29	1.688	20.69
6.94	1.811	14.48	10.74	1.462	26.89
6.64	1.596	18.62	10.35	1.327	33.79
6.26	1.361	25.17	13.94	2.046	13.45
5.99	1.223	30.00	13.47	1.821	16.90
5.66	1.078	35.17	12.97	1.618	21.93
11.00	2.357	13.10	12.59	1.483	24.14

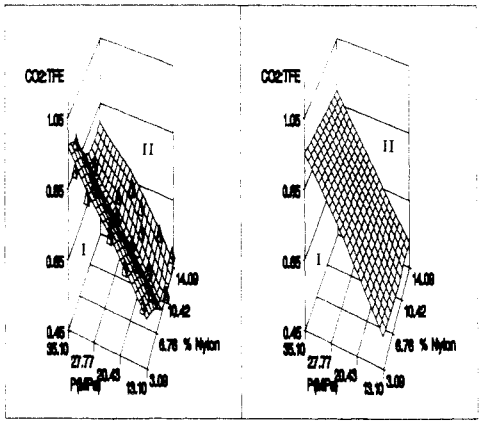

Figure 10. Liquid–liquid equilibrium phase surface (weight basis) for the Nylon 6/TFEtOH/CO_2 system at 373.15 K. The figure on the left represents the experimental data (Δ) and smoothed experimental phase surface (grids). The figure on the right represents SAFT predictions (grids). Region I consists of a single liquid phase. Region II consists of two phases (liquid–liquid).

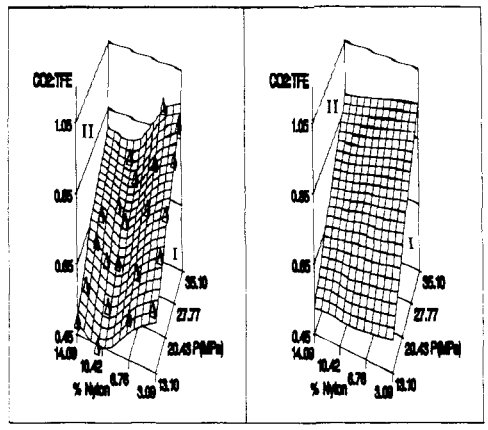

Figure 11. Liquid–liquid equilibrium phase surface (weight basis) for the Nylon 6/TFEtOH/CO_2 system at 373.15 K. The figure on the left represents the experimental data (Δ) and smoothed experimental phase surface (grids). The figure on the right represents SAFT predictions (grids). Region I consists of a single liquid phase. Region II consists of two phases (liquid–liquid).

Nylon 6. However, a rotated version of the phase surface (Figure 11) shows that the allowable amount of CO_2 in the single-phase region decreases initially, reaches a minimum, and later increases with increasing Nylon 6 concentration. This feature indicates an optimum region in the phase diagram (the minima) wherein the addition of CO_2 enhances the solubility of Nylon 6, thus suggesting a cosolvent effect.

SAFT *predicts* the phase behavior of the Nylon 6/TFEtOH/CO_2 system quite satisfactorily, with the notable exception of reproducing the minimum. It must be noted that all adjustable parameters were obtained from Table 4 and were not adjusted to fit the liquid–liquid equilibrium data for this system. In other words, the TFEtOH/CO_2 interaction parameter was obtained from an analysis of binary density data, the Nylon 6/TFEtOH interaction parameter was obtained from binary solid–liquid equilibrium data, and the Nylon 6/CO_2 interaction parameter was obtained from ternary Nylon 6/TFEtOH/CO_2 solid–liquid equilibrium data. At low CO_2 concentrations and low pressure, only two phases are predicted, a TFEtOH-rich liquid phase, which includes most of the Nylon 6, and a CO_2-rich fluid phase containing sparing amounts of Nylon 6. As the CO_2 concentration increases, SAFT predicts the onset of a second liquid phase, which is comprised of a mixture of TFEtOH, CO_2, and a small quantity of Nylon 6 whose composition is higher than the fluid phase composition but lower than the TFEtOH-rich liquid phase composition. As the pressure is increased above the three-phase pressure, SAFT predicts the appearance of a liquid–liquid cloud point. As the CO_2 content increases at constant Nylon 6 concentration, the liquid–liquid cloud-point pressure increases similar to the experimental trend, as shown in Figure 10. However, as seen in Figure 11, the allowable amount of CO_2 in the single-phase region decreases steadily with increasing Nylon 6 concentration at constant pressure, unlike the minima exhibited by the experimental data. At this level of investigation, it is not possible to attribute this limitation to any particular deficiency of SAFT. However, possible reasons could lie in (a) the exclusion of ring structures in Wertheim's association theory and (b) the possibility for CO_2 to form weakly bound complexes with TFEtOH and Nylon 6.

SLP, on the other hand, failed to predict a liquid–liquid phase separation at 373.15 K. It is likely that this limitation is due to inaccuracies in the physical contribution of SLP or due to the nature of assumptions in deriving the association theory.

Conclusions

The significant features of this study are as follows:

(1) Liquid–liquid phase separation in the Nylon 6/TFEtOH mixture could not be experimentally verified due to the formation of highly viscous solutions. However, both models (SLP and SAFT) correlated the solid–liquid equilibrium data quite accurately and subsequent predictions did not suggest the occurrence of liquid–liquid phase separation at temperatures ranging from 298 to 493 K.

(2) TFEtOH and CO_2 are miscible in all proportions at temperatures below 373.15 K and pressures to 40 MPa. Both SAFT and SLP correlated the liquid densities of the TFEtOH/CO_2 mixture at 298.15 K and 6.98 MPa quite accurately. The SLP model indicates some cross-association between TFEtOH and CO_2, while SAFT does not indicate any complex formations with CO_2.

(3) The Nylon 6/TFEtOH/CO_2 ternary system at 298.15 and 318.15 K exhibits a metastable region, where the time for gelation (phase separation) depends on the Nylon 6 composition and temperature. CO_2 is a useful diluent for Nylon 6/TFEtOH mixtures at low Nylon 6 compositions (less than 4 wt %), as large amounts of CO_2 can be added while maintaining reasonable Nylon 6 solubility. SAFT correlates the phase equilibrium data quite satisfactorily. SLP, on the other hand, overestimates the CO_2 content at low Nylon 6 concentrations. Interestingly, the SLP model predicts a cosolvent effect due to CO_2 at high Nylon 6 concentrations, an effect which could not be verified experimentally due to high solution viscosities. The SLP model also indicates a weak cross-association between CO_2 and Nylon 6, similar to the observations for the TFEtOH/CO_2 mixtures.

(4) At 373.15 K and high CO_2 concentrations, the ternary system indicates liquid–liquid phase separation. The liquid–liquid cloud-point pressure increases with increasing CO_2 content at constant Nylon 6 concentration. CO_2 behaves as an excellent diluent in regions where (a) Nylon 6 concentration is high and (b) Nylon 6 concentration is low, similar to the experimental results obtained at 298.15 and 318.15 K.

SAFT predicts liquid–liquid phase separation at 373.15 K, while SLP failed to indicate any LLE. The dependence of the liquid–liquid cloud-point pressure on the CO_2 content at constant Nylon 6 content in the system was similar to the observed experimental results: as CO_2 content increased, cloud-point pressure increased. However, SAFT predicts a steady increase in the absorbed amount of CO_2, unlike the minima exhibited by the experimental data, with a decrease in the Nylon 6 concentration at constant pressure.

In summary, while SAFT represents the multiphase equilibrium of the Nylon 6/TFEtOH/CO_2 system quite accurately over a wide range of compositions, temperatures, and pressures, the SLP model is inaccurate in the correlation of solid–liquid equilibria of the ternary system at low Nylon 6 concentrations and temperatures below 318.15 K and fails to represent LLE at 373.15 K. Neither model could be verified at high Nylon 6 concentrations and temperatures below 315.15 K since experimental data could not be obtained at these conditions owing to high viscosity problems.

Acknowledgment. Funding provided by DuPont is gratefully acknowledged. We thank Mark Stocks, who

performed the DSC analysis on the TFEtOH/Nylon 6 system, Yvette Burnworth, who performed the vapor pressure experiments for TFEtOH, and Boris Veytsman for useful discussions.

References and Notes

(1) Aharoni, S. M.; Cilurso, F. G.; James, M. *J. Appl. Polym. Sci.* **1985**, *30*, 2505.
(2) Alder, B. J.; Young, D. A.; Mark, M. A. *J. Chem. Phys.* **1972**, *56*, 3013.
(3) Baur, E.; Namek, M. *Helv. Chim. Acta* **1940**, *23*, 1101.
(4) Brandrup, J.; Immergut, E. H. *Polymer Handbook*; Wiley-Interscience: New York, 1988.
(5) Carnahan, N. F.; Starling, K. E. *J. Chem. Phys.* **1969**, *51*, 635.
(6) Chapman, W. G.; Jackson, G.; Gubbins, K. E. *Mol. Phys.* **1988**, *65*, 1057.
(7) Chapman, W. G.; Gubbins, K. E.; Jackson, G.; Radosz, M. *Ind. Eng. Chem. Res.* **1990**, *29*, 1709.
(8) Coan, C. R.; King, A. D., Jr. *J. Am. Chem. Soc.* **1971**, *93*, 1857.
(9) Daubert, T. E.; Danner, R. P. *Data compilation: Tables of properties of pure compounds*: AIChE: New York, 1985.
(10) Economou, I.; Donohue, M. D. *AIChE J.* **1991**, *37*, 1875.
(11) Francis, A. W. *J. Phys. Chem.* **1954**, *58*, 1099.
(12) Garcia, D.; Starkweather, H. W., Jr. *J. Polym. Sci., Polym. Phys. Ed.* **1985**, *23*, 537.
(13) Gaur, U.; Lau, S.; Wunderlich, B. B.; Wunderlich, B. *J. Phys. Chem. Ref. Data* **1983**, *12*, 65.
(14) Ghonasgi, D.; Chapman, W. G. *Mol. Phys.*, in press.
(15) Gupta, R. B.; Combes, J. R.; Johnston, K. E. *J. Phys. Chem.* **1993**, *97*, 707.
(16) Gupta, S. K.; Lesslie, R. D.; King, A. D., Jr. *J. Phys. Chem.* **1973**, *77*, 2011.
(17) Hemmaplardh, B.; King, A. D., Jr. *J. Phys. Chem.* **1972**, *76*, 2170.
(18) Hempel, W.; Seidel, J. *Berichte* **1898**, *31*, 3000.
(19) Hildebrand, J. H.; Scott, R. L. *The solubility of nonelectrolytes*; Reinhold: New York, 1964; p 248.
(20) Hoefling, T. A.; Enick, R. M.; Beckman, E. J. *J. Phys. Chem.* **1991**, *95*, 7127.
(21) Huang, S. H.; Radosz, M. *Ind. Eng. Chem. Res.* **1990**, *29*, 2284.
(22) Huang, S. H.; Radosz, M. *Ind. Eng. Chem. Res.* **1991**, *30*, 1994.
(23) Joesten, M. D.; Schaad, L. J. *Hydrogen Bonding*; Marcel Dekker Inc.: New York, 1974.
(24) Kholafa, J.; Nezbeda, I. *Mol. Phys.* **1987**, *61*, 161.
(25) Kohan, M. I. *Nylon Plastics*; John Wiley and Sons: New York, 1973.
(26) Krigbaum, W. R.; Carpenter, D. K. *J. Polym. Sci.* **1954**, *14*, 241.
(27) Levine, S.; Perram, J. W. In *Hydrogen-bonded Solvent Systems*; Covington, A. K., Jones, P., Eds.; Taylor and Francis: London, 1968.
(28) Lucchelli, I. T.; Vansco, G.; Yeh, P. L. *Polym. Bull.* **1988**, *20*, 569.
(29) MacKnight, W. J.; Yang, M. *J. Polym. Sci., Polym. Symp.* **1973**, *42*, 817.
(30) Nezbeda, I.; Kolafa, J.; Kalyuzhnyi, Y. J. *Mol. Phys.* **1989**, *68*, 143.
(31) Ohgaki, K.; Katayama, T. *J. Chem. Eng. Data* **1976**, *21*, 53.
(32) Panayiotou, C. *Fluid Phase Equilib.* **1988**, *92*, 2960.
(33) Panayiotou, C. *Pure Appl. Chem.* **1989**, *61*, 1453.
(34) Panayiotou, C. *Fluid Phase Equilib.* **1990**, *56*, 171.
(35) Panayiotou, C.; Sanchez, I. C. *J. Phys. Chem.* **1991**, *95*, 10090.
(36) Perry, R. H.; Chilton, C. H. *Chemical Engineers' Handbook*, 5th ed.; McGraw-Hill Co.: New York, 1973; pp 3–227.
(37) Pimental, G. C.; McClellan, A. L. *The hydrogen bond*; Freeman: San Francisco, CA, 1960.
(38) Sanchez, I. C.; Lacombe, R. H. *J. Phys. Chem.* **1976**, *80*, 2352.
(39) Sanchez, I. C.; Lacombe, R. H. *Macromolecules* **1978**, *11*, 1145.
(40) Schroeder, L. R.; Cooper, S. L. *J. Appl. Phys.* **1976**, *47*, 4310.
(41) Starkweather, H. W.; Jones, G. A. *J. Polym. Sci., Polym. Phys. Ed.* **1981**, *19*, 467.
(42) Suresh, S. J.; Elliott, J. R., Jr. *Ind. Eng. Chem. Res.* **1992**, *31*, 2783.
(43) Vargaftik, N. B. *Tables on the thermophysical properties of liquids and gases*; John Wiley and Sons, Inc.: New York, 1975.
(44) Veytsman, B. A. *J. Phys. Chem.* **1990**, *94*, 8499.
(45) Walsh, J. M.; Guedes, H. R.; Gubbins, K. E. *J. Phys. Chem.* **1992**, *96*, 10995.
(46) Wertheim, M. S. *J. Stat. Phys.* **1984**, *35*, 19.
(47) Wertheim, M. S. *J. Stat. Phys.* **1984**, *35*, 35.
(48) Wertheim, M. S. *J. Stat. Phys.* **1986**, *42*, 459.
(49) Wertheim, M. S. *J. Stat. Phys.* **1986**, *42*, 477.
(50) Xenopoulos, A.; Wunderlich, B. *J. Polym. Sci., Polym. Phys. Ed.* **1990**, *28*, 2271.

Author Supplied Registry No. 1, 25038-54-4.